Separation Science and Technology
Publication details, including instructions for authors and subscription information:
http://www.informaworld.com/smpp/title~content=t713708471

Microfiltration of Protein Precipitate from Clarified Yeast Cell Homogenate for the Recovery of a Soluble Product

J. A. Levesley[ab]; M. Seggianni[a]; M. Hoare[a]
[a] DEPARTMENT OF CHEMICAL AND BIOCHEMICAL ENGINEERING, ADVANCED CENTRE FOR BIOCHEMICAL ENGINEERING, UNIVERSITY COLLEGE LONDON, LONDON, UK [b] Industrial Research Limited, Lower Hutt, New Zealand

Online publication date: 04 March 2000

To cite this Article Levesley, J. A. , Seggianni, M. and Hoare, M.(2000) 'Microfiltration of Protein Precipitate from Clarified Yeast Cell Homogenate for the Recovery of a Soluble Product', Separation Science and Technology, 35: 5, 633 — 649
To link to this Article: DOI: 10.1081/SS-100100181
URL: http://dx.doi.org/10.1081/SS-100100181

SEPARATION SCIENCE AND TECHNOLOGY, **35**(5), pp. 633–649, 2000

Microfiltration of Protein Precipitate from Clarified Yeast Cell Homogenate for the Recovery of a Soluble Product

J. A. LEVESLEY,* M. SEGGIANNI, and M. HOARE
DEPARTMENT OF CHEMICAL AND BIOCHEMICAL ENGINEERING
ADVANCED CENTRE FOR BIOCHEMICAL ENGINEERING
UNIVERSITY COLLEGE LONDON
LONDON, WC1E 7JE, UK

ABSTRACT

A crossflow microfiltration unit was used to recover the soluble proteins from a protein precipitate suspension prepared from disrupted yeast. The effects of the process parameters transmembrane pressure (TMP), crossflow velocity, and suspension concentration on the permeate flux and transmission (sieving coefficient) of soluble proteins were determined. Flux increased with increasing crossflow velocity and decreasing concentration, and increased with increasing TMP up to a critical value at which the flux became independent of pressure. Protein transmission also increased with increasing crossflow and decreasing concentration, but had a maximum value at a critical TMP, near the critical value for flux, and declined at higher pressures. A simple analysis based on film theory indicated that the pattern of variation in measured transmission (i.e., permeate protein concentration divided by feed protein concentration) with increasing TMP was due to two competing factors: increasing protein concentration at the membrane surface and decreasing intrinsic transmission (i.e., transmission calculated with respect to the concentration at the membrane surface). Although flux and transmission both increased with decreasing concentration, it was found that an intermediate concentration gave the best rate of soluble protein recovery. Differences were also noted between the transmission of a target enzyme, alcohol dehydrogenase (ADH), and the overall transmission of total soluble protein.

* To whom correspondence should be addressed at Industrial Research Limited, PO Box 31–310, Lower Hutt, New Zealand. Telephone: +64 4 569 0000 ext. 4048. FAX: +64 4 569 0132. E-mail: j.levesley@irl.cri.nz

INTRODUCTION

Recovery of intracellular protein from fermentation broths is a common task in biotechnology industries. For a typical process, the microbes are harvested by centrifugation or microfiltration, resuspended in buffer, homogenized to release the product, and then the suspension is clarified to remove cell debris (1) On an industrial scale, fractional protein precipitation is an important operation for selectively recovering a target protein from the clarified solution (2). Recovery of the enzyme alcohol dehydrogenase (ADH) from baker's yeast has been chosen as a model system for this process at the Advanced Centre for Biochemical Engineering, UCL (2). The work presented here concerns the use of crossflow microfiltration for the clarification of the protein solution following the first precipitation step in a two-step process; the stage at which the target protein is in solution and contaminants of lower solubility have been precipitated.

Efficient soluble protein recovery by microfiltration requires high rates of permeate flux and target protein transmission, with high retention of solids. These objectives are achievable, but performance declines with time due to concentration polarization and membrane fouling, leading to lower fluxes and transmissions (3). A correct choice of operating parameters is necessary for performance at acceptable levels. The work here focuses on the effects of three operating parameters: feed concentration, crossflow rate, and transmembrane pressure (TMP) on the membrane process performance, i.e., on permeate flux and protein transmission. A good summary of the literature and an investigation of the effects of the same operating parameters on the similar problem of the microfiltration of bacterial cell lysate can be found in Parnham and Davis (1). There appears to be little published on microfiltration of protein precipitates other than that of Bentham et al. for soya protein (4).

The economic performance of a process may be considered in terms of the mass flux of target protein and its concentration in the permeate. The relationship between these performance measures and permeate flux and protein transmission is also investigated here, as the conditions for optimizing the two sets of performance measures may not coincide.

MATERIALS AND METHODS

Preparation of Protein Precipitate Suspension

A 50% w/v suspension of baker's yeast (*Saccharomyces cerevisiae*) was prepared by suspending packed yeast (DCL Ltd., Crawley, UK) in 0.02 M phosphate buffer at pH 6.5 (1.5 kg of packed yeast in 1.5 L of buffer). The suspension was homogenized at 10°C using a high-pressure homogenizer (Lab 60, APV Manton-Gaulin, Crawley, UK) using 5 passes at 500 bar. The ho-

mogenate was then diluted with an equal volume of phosphate buffer to give a 25% w/v suspension which was clarified using a tubular bowl centrifuge (Sharples 1P) at 45,000 rpm. A saturated ammonium sulfate solution was added to the supernatant to give a final concentration of ammonium sulfate of 40%. This suspension was stored frozen at −20°C in 1 L aliquots until use.

Before use, the 40% ammonium sulfate suspension was defrosted, then stirred at 250 rpm in a 1.4-L tank at 4°C for 40 minutes to allow precipitate formation and aging for maximum precipitate size (2). For one set of experiments, three lower concentrations were each made by dilution of a batch of original suspension with additional 40% ammonium sulfate solution to concentrations of 1/2, 1/5, and 1/10 by volume.

Crossflow Filtration Apparatus

Microfiltration was carried out using a small-scale crossflow module, the Mini-Ultrasette (Pall-Filtron). The device had a filtration area of 0.005 m^2 and an open-channel configuration with a channel height of 0.76 mm and breadth of 30 mm. It was fitted with a low protein binding "Omega" membrane (polyethersulfone) with nominal pore size of 0.16 μm. Crossflow was provided by a gear pump equipped with a variable speed drive (Ismatec, Surrey, UK) connected to the device by flexible tubing. A screw clamp on the retentate return tubing generated backpressure within the device, producing a permeate flow. A pressure gauge on the retentate return line was used to measure the outlet pressure. The outlet pressure was taken to be a measure of the average feed side pressure since the pressure drop from inlet to outlet of the module was previously measured to be negligible (<0.05 bar) at the flow rates used. It was also taken to be equal to the transmembrane pressure (TMP) since the permeate side was open to atmosphere. The pump speed was adjusted where necessary to maintain the set flow rate when the backpressure was adjusted.

Operating Procedures

The suspension was circulated at room temperature (22–24°C) at a flow rate of 400, 500, or 600 mL/min with a transmembrane pressure in the 0.5 to 2.25 bar range. The corresponding crossflow velocities were calculated to be 0.29, 0.37, and 0.44 m/s, respectively, and the flow was laminar at all recirculation rates. The permeate was returned to the feed tank at regular intervals to keep the feed concentration constant. Samples were taken from the retentate return line every 10 minutes and from the permeate every 5 minutes, and stored on ice until the end of the experiment. In experiments where pressure was altered during a run, 30 minutes of constant pressure were maintained before an approximately "steady-state" value of flux and transmission was determined.

Permeate and crossflow rates were measured by timing the flow into measuring cylinders.

Cleaning of the module was in accordance with the manufacturers instructions, with 0.1 N NaOH solution recirculated for a total of 1 hour, and then the system was flushed with deionized water until the pH of the rinsewater was neutral. If a water flux of 50–90% of the original value was not achieved, then the above procedure was repeated with a more concentrated NaOH solution, up to 1 N.

Assays

The retentate and permeate samples were assayed for total protein and for the enzyme alcohol dehydrogenase (ADH). Total protein concentration was determined using the Bradford assay (Bio-Rad Laboratories Ltd.) and the activity concentration of ADH using the method of Bergmeyer (5, 6). The retentate samples were spun down in a microcentrifuge at 13,000 rpm. for 10 minutes and the assay sample was taken from the supernatant. The retentate concentrations calculated were therefore with respect to the liquid fraction of the retentate and so no correction had to be made for solids content when calculating the transmission values.

RESULTS

The Effect of Concentration on Flux and Transmission Profiles

Figure 1 shows the flux decline curves with time for four fractional precipitate suspensions at different concentrations. Permeate flux was calculated by dividing the permeate volume flow rate (L/h) by the membrane area (m^2). The resultant concentration of each suspension is given in terms of total soluble protein measured in the feed. In each experiment the feed was circulated at 400 mL/min and the transmembrane pressure (TMP) was 1 bar. It can be seen that flux declined rapidly with time initially and reached a quasi-steady state after approximately 30 minutes. Flux increased with decreasing concentration.

Figure 2 shows the change of transmission with time of total protein and of ADH at different concentrations from the same experiments as shown in Fig. 1. Transmission was calculated by dividing the protein concentration or ADH activity in the permeate samples by the average of the corresponding value in the retentate samples. Retentate levels were approximately constant throughout each run. Levels of ADH were too low to be measured accurately at the lower concentrations, so only the two higher concentrations are shown. As with flux, transmission declined with time to a quasi-steady state and these

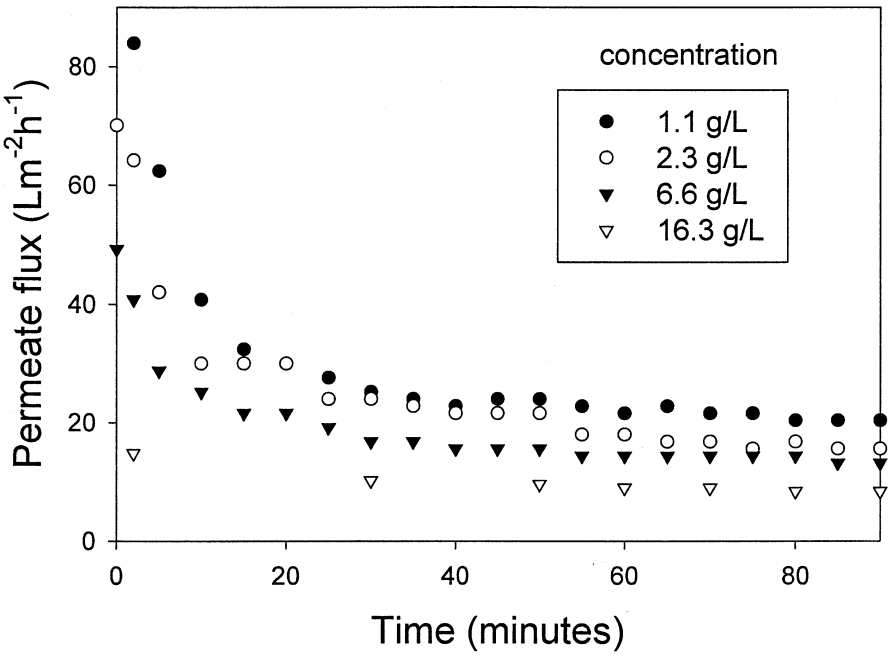

FIG. 1 Effect of feed concentration on permeate flux–time profiles. Crossflow = 0.29 ms^{-1}, TMP = 1 bar. Total soluble protein concentration in feed given in the inset.

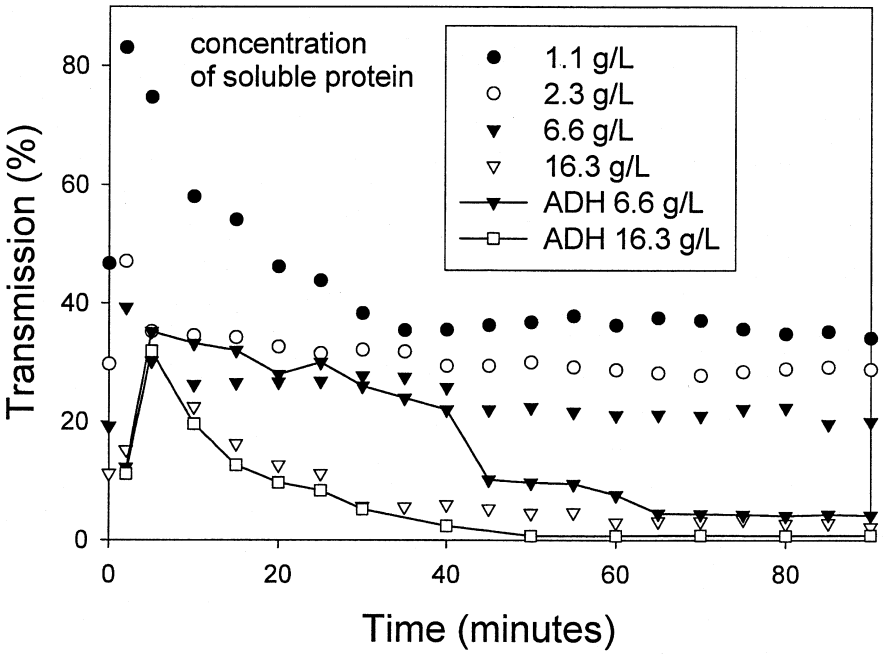

FIG. 2 Effect of feed concentration on total soluble protein and ADH transmission–time profiles. Crossflow = 0.29 ms^{-1}, TMP = 1 bar. Total soluble protein concentration in feed given in the inset. (ADH transmission only given for the two highest concentration feeds.)

transmission values increased with decreasing concentration. The transmission of ADH is initially similar to that of total protein but declined gradually to less than half of the total protein value. The apparent initial rise in transmission values is thought to be an artifact reflecting the dilution of the first permeate sample by the water initially filling the permeate side.

The Effect of Transmembrane Pressure and Crossflow on Flux and Transmission

The effects of TMP on permeate flux for fractional precipitate suspensions are shown in Fig. 3 for three different crossflow rates. The suspensions were all at the original concentration, with an average soluble protein concentration of 17.8 g/L and ADH activity of 124 U/mL. The results at each pressure were obtained after filtration under constant conditions for 30 minutes in order to obtain a quasi-steady state, then the pressure was increased to the next higher value. It can be seen that the curves change from a pressure-dependent flux to an almost pressure-independent flux at approximately 1.25 bar. They also show increasing flux with increasing crossflow, particularly in the pressure-independent region.

Figures 4 and 5 show the transmission of total soluble protein and of ADH, respectively, taken from the same experiments as shown in Fig. 1. For both to-

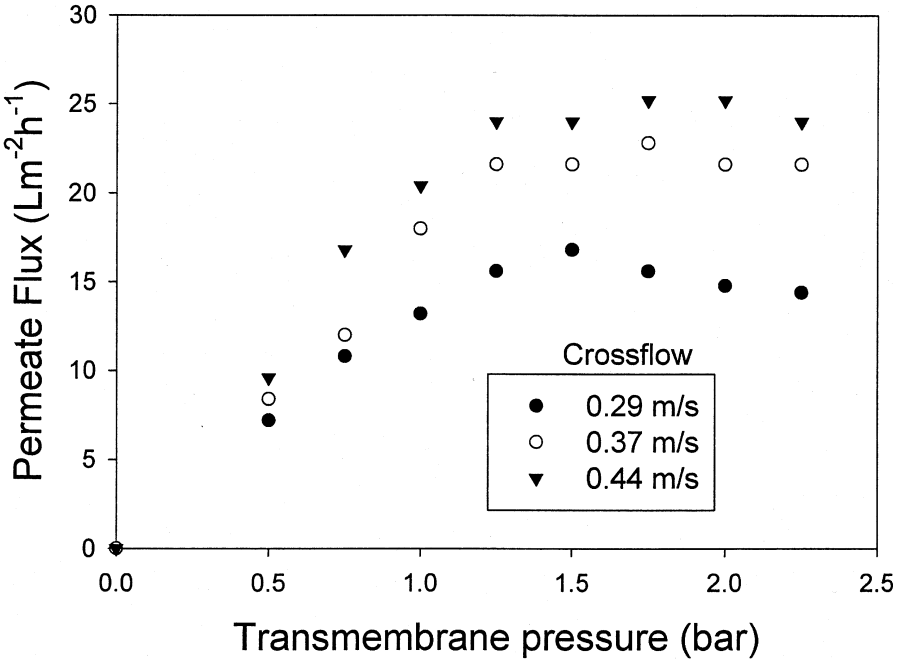

FIG. 3 Steady-state flux as a function of pressure for various crossflow rates. Full concentration feeds (average 17.8 g/L total soluble protein).

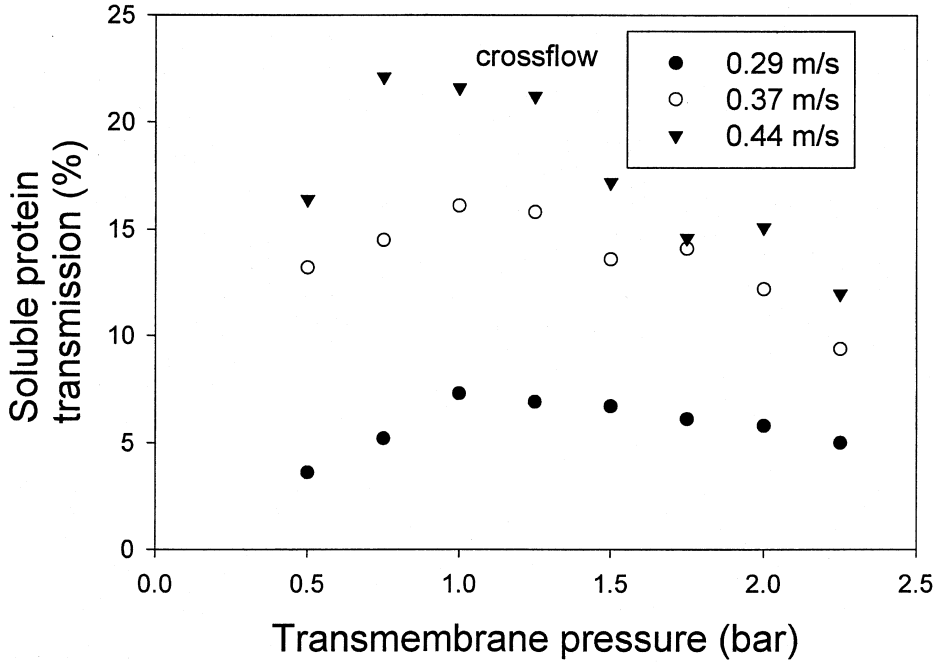

FIG. 4 Steady-state total soluble protein transmission as a function of pressure for various crossflow rates. Full concentration feeds (average 17.8 g/L total soluble protein).

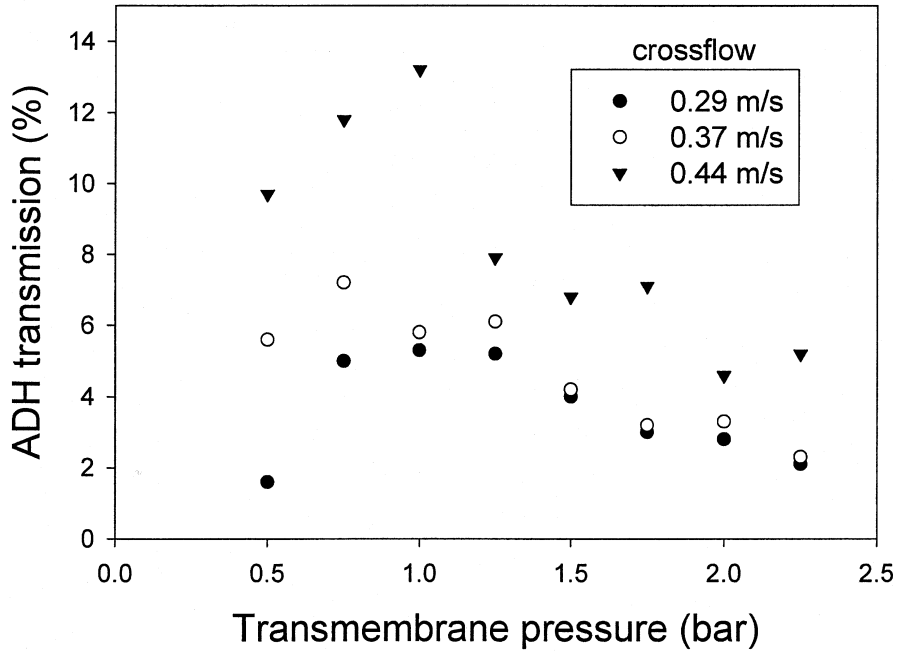

FIG. 5 Steady-state ADH activity as a function of pressure for various crossflow rates. Full concentration feeds (average 17.8 g/L total soluble protein).

tal protein and for ADH, transmission increased with increasing pressure up to about 1 bar and then decreased with further increases in pressure. The figures also show that the transmissions increased with increasing crossflow.

DISCUSSION

Effect of Process Parameters on Flux

The flux decline with time and the steady-state responses of the flux to changes in concentration, crossflow, and transmembrane pressure seen in Figs. 1 and 3 are all qualitatively in agreement with many previously reported studies of microfiltration (6–8). Flux decline with time is generally due to a combination of concentration polarization, cake formation, and membrane fouling (7). The flux decline with increasing TMP seen above 1.75 bar for the lowest crossflow, 0.29 m/s, has also been reported in the literature (9) and may be interpreted as increased fouling resistance due to increased pore blocking (7).

The existence of a pressure-independent flux region is also a widely reported result in the literature (9). The limiting flux almost always increases with increasing crossflow, as it did here (6). The limiting flux has been considered to be due to the formation of a "gel layer" of solutes or a thickening cake layer of solids, once the surface concentration has reached a physical maximum (9). It may be noted that other models for limiting flux with solutes exist which do not involve a maximum or gel concentration such as the osmotic pressure model (10) and the concentration-dependent viscosity (11), but the gel theory is the most convenient to use here. It may be considered as a limiting case of the film model which is discussed further below.

The effects of changing crossflow on flux shown in Fig. 3 are most readily understood as producing changes in the mass transfer coefficient defined in the film model of crossflow filtration. The film model may be written as (12)

$$J = k \ln\left(\frac{C_w - C_p}{C_b - C_p}\right) \tag{1}$$

where J is the permeate volume flux, k is the mass transfer coefficient, C_b is the bulk concentration, C_w is the wall concentration (i.e., at the membrane surface), and C_p is the permeate concentration.

Many correlations exist for the mass transfer coefficient, k, as a function of crossflow velocity, U, for simple solutions of solutes or of solids (7, 9, 12). These are in the form

$$k = k' U^n \tag{2}$$

where U is the average crossflow velocity, k' is a constant of proportionality depending on the feedstream properties and filter geometry, and n is the ex-

MARCEL DEKKER, INC.
270 Madison Avenue, New York, New York 10016

ponent of crossflow. The value of n remains the same if the equation is written in terms of the wall shear rate, γ, which is directly proportional to U.

There is no general agreement on a single correct value for the exponent n in crossflow microfiltration, although in ultrafiltration the Lévêque solution in laminar flow is often used, which gives $n = 1/3$ (9). Modified theories for the filtration of suspended solids include shear-induced diffusion (13) and inertial lift (14) which predict the exponent n to be 1 and 2, respectively, whereas experimentally determined correlations have been found with exponents ranging from 0.15 to 1.09 for the microfiltration of microbial suspensions (15). Furthermore, it has been pointed out (16) that no general expressions exist for predicting flux for mixtures of solids and solutes. To find the values for the constants k' and n in the present work, and thus compare them with previously reported studies, Eqs. (1) and (2) were combined to give

$$J = k' U^n \ln\left(\frac{C_w - C_p}{C_b - C_p}\right) \tag{3}$$

Taking the results of the experiments shown in Fig. 3 at TMP = 1.25 bar, the correlation between flux and crossflow was found to give n approximately equal to 1. This is in agreement with the shear-induced diffusion theory (13), suggesting that the precipitate particles control the flux, although there are too few data points to make a definite conclusion. The value of $n = 1$ also matches the results for ultrafiltration of soya protein precipitates at low crossflows (16). The calculation is explained in more detail in the following section.

The increases in steady-state flux with decreasing bulk concentration shown in Fig. 3 are in accordance with the film model for crossflow filtration according to Eq. (3) as well as with previous reports (7).

Calculation of Parameters for the Film Model

According to the "gel model," it is assumed that the wall concentration has reached a maximum (a gel for solutes, a cake for solid particles) in the pressure-independent region. This maximum value, C_{max}, can be extrapolated from experimental data at different concentrations, and then values for k' and n are found to fit Eq. (3) from results at different crossflows. These calculations were carried out for the present data as described below. It should be noted that the calculations were based on the concentration of total soluble protein because predictions of protein concentration at the wall were needed in order to reexamine the protein transmission data. This does not necessarily imply that the concentration of soluble protein itself was thought to be at a physical maximum in the pressure-independent flux region. The flux could equally be limited by the solid particles forming a cake, or by some combination of solids and solutes. Whatever is actually limiting the flux, the mass balance described in the film model requires that, for the soluble protein compo-

nent as for any component, a constant, maximum flux implies a constant, maximum wall concentration under the given conditions.

The values of the flux at 30 minutes were plotted against the log of the difference between the bulk and permeate concentrations taken from the experiments shown in Fig. 1. The concentrations were taken throughout to be the concentration of total soluble protein. A best fit straight line through the points was extrapolated to zero flux. According to Eq. (1), at zero flux, $C_b = C_w$ and we assume that $C_w = C_{max}$ in the pressure-independent region. The intercept was found to be at a concentration of $C_b = C_{max} = 129$ g/L soluble protein. (This assumes C_p is neglible at $C_b = C_{max}$, a reasonable assumption since $C_p = 0.057C_b$ at 16.3 g/L, and the fraction declines with increasing concentration. Another small source of error is that the data were taken with the pressure just below the pressure-independent region, at 1 bar.)

Given an estimated value for $C_w = C_{max} = 129$ g/L in the pressure-independent region, then data at different flow rates, q, may be used to estimate the values of k' and n in Eq. (3). The flux and bulk and permeate concentration values were taken from the experiments shown in Figs. 3 and 4 with the pressure at 1.25 bar. Pressure-independent flux divided by the natural log term of Eq. (3) was plotted against crossflow velocity on logarithmic axes. The best fit straight line through the data had a gradient of 1.03 with a correlation coefficient (R^2) of 0.94. According to Eq. (3), the gradient of this log-log plot corresponds to the value of n, i.e., $n = 1.03$. It was decided to force the value of n to be 1 for simplicity in subsequent calculations. With $n = 1$, Eq. (3) predicts that flux divided by the log term should be directly proportional to the crossflow velocity. A reasonable fit between this model and the data was found as shown in Fig. 6. Flux, J, has been converted from units of L/m^2/h into units of m/s so that k' is nondimensional. The slope of the best fit line and hence the corresponding value of k' was 7.0×10^{-6}.

These values of $C_{max} = 129$ g/L, $n = 1$, and $k' = 7.0 \times 10^{-6}$ are only indicative, based on a limited data set, but are useful for a qualitative analysis of the effect of pressure and crossflow on intrinsic transmission. It should also be noted that the value of C_{max} does not necessarily represent a physical maximum (gel) concentration for the soluble proteins, as discussed above.

Effect of Process Parameters on Transmission

The effect of process parameters on transmission has not been so well documented in the literature on microfiltration, and there are no generally accepted theoretical expressions for correlating transmission with these parameters in the filtration of realistic process streams. Treatments do exist for dilute solutions of pure proteins in ultrafiltration (17). The results of Fig. 2 show transmission increasing with decreasing concentration, which is in agreement with a report on the microfiltration of cell debris (1), although another report

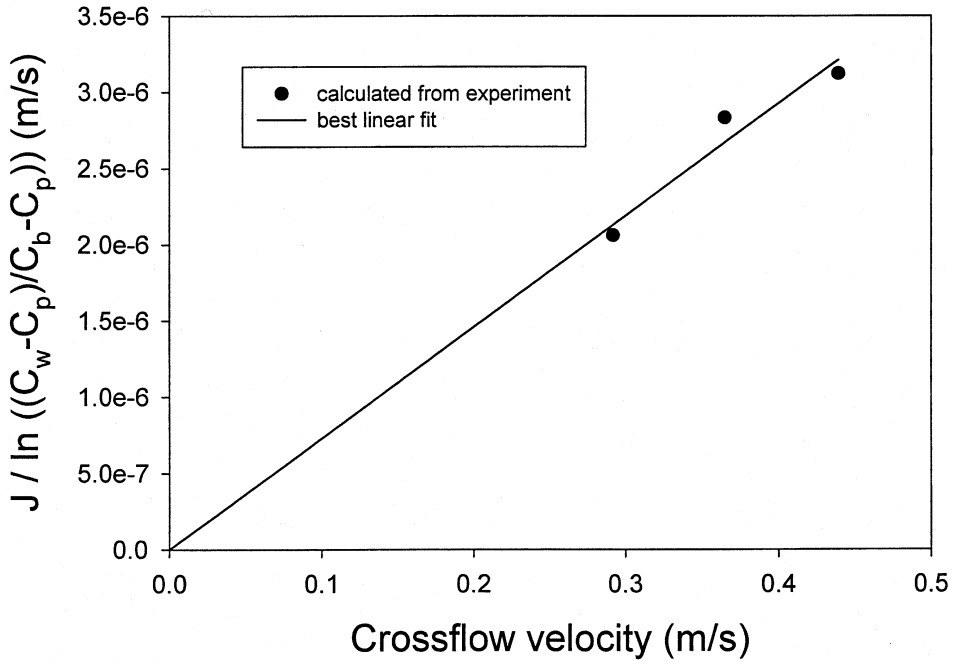

FIG. 6 Flux, J, divided by $1n[(C_w - C_p)/(C_b - C_p)]$ plotted against crossflow velocity for pressure-independent fluxes, with a best fit straight line through the origin. Direct proportionality is predicted by putting $n = 1$ in the film model, Eq. (3).

has found transmission to be insensitive to changes in concentration of a fermentation broth (18).

Figures 4 and 5 show increasing transmission with increasing crossflow. Increasing crossflow would intuitively be expected to increase transmission as it increases flux by clearing the membrane surface. The literature does in fact show the effect of increasing crossflow to be positive in most cases [1 (at low concentrations), 19, 20, 21 (at high TMP), 22], though sometimes the effect is neutral [8, 1 (at high concentrations), 20 (clarified feedstreams), 23, 21 (at low TMP)].

Figures 4 and 5 also show the existence of a peak in transmission at around 1 bar TMP. This does not seem to have been previously reported in literature on microfiltration of biological feedstreams. Transmission is generally reported to decrease with increasing TMP (8, 24, 18, 23), though it may increase [25, 20, 22 (at low crossflow velocities)] or stay constant [1, 4, 22 (at high crossflow velocities)].

A possible explanation for the rise and subsequent fall of observed transmission with increasing TMP is that it is the combination of two effects: a rise in wall concentration as polarization increases and a fall in intrinsic transmission (the permeate concentration as a fraction of the wall concentration). This approach has been used to explain a minimum (fall then rise) in observed

transmission with increasing TMP for dilute solutions of macrosolutes (26). The explanation is discussed further below.

Interpretation of the Observed Transmission Profiles in Terms of Intrinsic Transmission

The transmission shown in Figs. 2, 4, and 5 is the observed, or "extrinsic," transmission, i.e., the concentration of soluble material (or activity concentration for ADH) in the permeate divided by its concentration in the bulk of the retentate. More insight into the behavior of the membrane and the polarized layers comes from considering the true, or "intrinsic," transmission which uses the concentration of soluble material next to the filtering surface, rather than the bulk concentration. The intrinsic transmission therefore gives the fraction of the material actually available at the surface which passes through into the permeate.

Although the wall concentration, C_w, cannot usually be measured directly, an estimate of its value may be made by using the simple film theory as given in Eq. (3). The values of $n = 1$, and $k' = 7.0 \times 10^{-6}$ derived from the flux data as shown above were substituted into Eq. (3) along with the measured values of J, C_b, and C_p from the experimental results shown in Figs. 3 and 4.

The results of the calculations of C_w for soluble protein are shown in Fig. 7. The wall concentration at zero TMP, hence zero flux, has been set equal to the bulk concentration for each experiment in accordance with Eq. (1). The fit is fairly close to the predicted maximum concentration of 129 g/L at pressures at and above the critical value of 1.25 bar for all three crossflow velocities. Since the maximum concentration was predicted only from data taken at 0.29 m/s, and from different experiments to those used here, the reasonable fit supports the use which was made of the "film-gel model" with soluble protein concentration data. The decline in calculated wall concentration for the 0.29 m/s crossflow run above 1.5 bar is a result of the decline in flux due to fouling which is not accounted for in the model. The most interesting feature of the graph is that it shows how C_w is calculated to vary in the pressure-dependent flux region, below 1.25 bar. Here it increases almost linearly with increasing TMP and is not a strong function of crossflow rate.

The resultant intrinsic transmissions for total soluble protein were calculated by dividing the measured value of C_p by the calculated C_w and are shown in Fig. 8. The intrinsic transmission is seen to decline with increasing TMP across the whole range of pressures for the higher crossflows and to decline or stay constant at the lowest crossflow. Comparison between Fig. 4, showing extrinsic transmission, and Fig. 8 indicates that the rise in observed (extrinsic) transmission at lower pressures was due to the fact that the rise in wall concentration with increasing TMP (hence flux) overcompensated for a fall in the

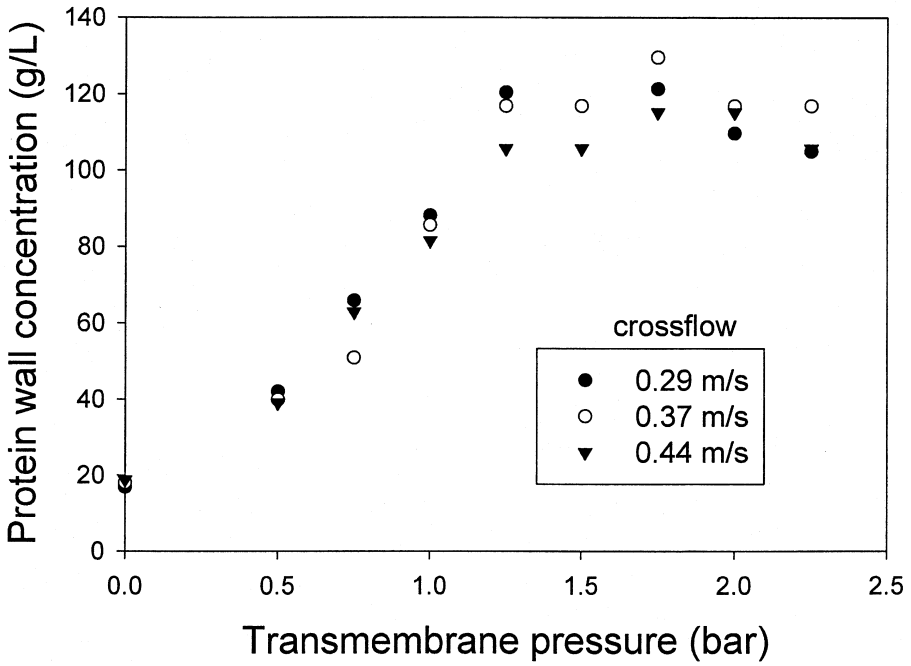

FIG. 7 Calculated values of wall concentration of soluble protein in the experiments shown in Figs. 3, 4, and 5. Calculated using Eq. (3) with experimental data for J, C_b, and C_p, and fitted values of the parameters k' and n.

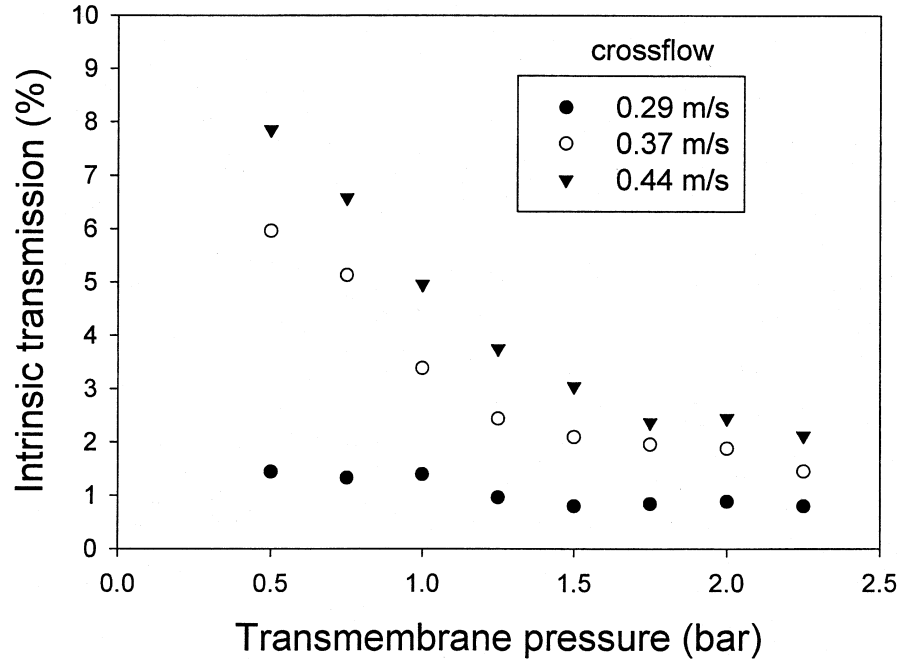

FIG. 8 Calculated values of intrinsic transmission as a function of TMP for various crossflow rates. Calculated using wall concentrations from Fig. 6 and experimental data from experiments shown in Figs. 3, 4, and 5.

MARCEL DEKKER, INC.
270 Madison Avenue, New York, New York 10016

true transmission of total protein. Then it appears that the fall in observed transmission at higher pressures was the result of the continued fall in intrinsic transmission with a constant wall concentration. Second, it can be seen that the increase in extrinsic transmission with increasing crossflow appears to reflect an increase in intrinsic transmission.

Optimization of the Process for Product Recovery

The effect of transmembrane pressure, crossflow velocity, and feed concentration are reexamined below for the impact on process performance as measured here by the protein flux ($g/m^2/h$). This represents the rate at which soluble protein is collected in the permeate per unit area of membrane, and it is calculated as the product of the concentration in the permeate and the permeate flux. Maximizing performance in terms of product flux will minimize the membrane area required for achieving a given product yield (recovered fraction of the available product) within a given process time. As a point of comparison, enzyme recovery from a fermentation broth was thought to be economically feasible at a flux of 40 $L/m^2/h$ and an enzyme transmission of 50% (27).

Ideally, the flux of the target enzyme, ADH, would be considered, but the data could not be collected for ADH transmissions at the lower concentrations so total protein data were considered. The qualitative conclusions reached for total protein would be expected to apply to ADH since the transmission data showed the same trends in the effects of pressure, crossflow, and concentration.

Since maximum transmission occurs at a TMP of 1 bar (Figs. 4 and 5) and maximum flux is achieved at 1.25 bar, with flux constant or declining above that pressure (Fig. 3), then it is clear that the optimum operating TMP is between 1 and 1.25 bar in this system. Both flux and transmission are increased by increasing the crossflow velocity, so maximum performance occurs at maximum crossflow velocity in this system.

It was also found that flux and transmission were increased by diluting the feedstream (Figs. 1 and 2) and were a maximum at the lowest concentration. Table 1 shows the flux and transmission of total protein after 30 minutes for those experiments. However, the table also shows that the 2:1 dilution (6.6 g/L total protein in the feed) gave the highest protein flux, which does not correspond with the maximum for either flux or transmission.

An important factor in the cost of further downstream processing is the total permeate volume (27). Permeate volume is minimized for a given yield by maximizing the permeate concentration. Table 1 shows that the 6.6 g/L feed also gave the maximum value for this performance measure. The optimum concentration will not necessarily coincide for the two performance measures as they have done in this case. (Note that the next highest permeate protein

TABLE 1
Process Performance Versus Feed Concentration
(data taken from experiments shown in Figs. 1 and 2 at time 30 minutes)

Feed protein concentration (g/L)	Permeate flux ($L/m^2/h$)	Observed transmission (%)	Protein flux ($g/m^2/h$)	Permeate concentration (g/L)
16.3	10.2	5.7	9.5	0.93
6.6	16.8	27.7	30.7	1.83
2.3	24	32.1	17.7	0.74
1.1	25.2	38.3	10.6	0.42

concentration was given by the 16.6 g/L feed, but that this feed concentration gave the lowest protein flux.)

Transmission of ADH Compared with Total Protein

Comparison of Figs. 4 and 5 indicates that the value of ADH transmission is approximately half that of the total soluble protein. Various factors could contribute to the relatively low transmission of ADH. Fundamental studies of pure ADH solutions have shown that nonideal pH and ionic conditions (pH 7.5, 10 mM buffer solution), such as are present in the precipitate solution, will lead to the aggregation of the ADH molecules to form large complexes and that the high concentrations will promote deposition on the membrane surface under the influence of shear (28).

It also may be noted from Fig. 2 that the ratio of ADH to total protein transmission is approximately 1 initially, but declines with time as the flux declines with increasing membrane fouling. A similar decline in the ratio of ADH to total protein transmission upon increased fouling has previously been noted for studies of microfiltration of yeast cell homogenate suspensions (29), where the change in selectivity was explained by the narrowing of effective pore diameter by membrane fouling.

CONCLUSIONS

Crossflow microfiltration has been examined at a small scale for the recovery of a soluble enzyme, ADH, from a protein precipitate suspension. The flux and transmission values at low crossflow velocity and high concentration were too low for a typical economically viable process. Increased crossflow produced increases in flux and transmission. Flux increased approximately linearly with crossflow, which was shown to correspond to the film model for filtration with shear-induced diffusion controlling mass transfer. Increasing

degrees of dilution of the feedstream also produced increases in flux and transmission, but an intermediate dilution was found to be optimum for maximizing the rate of soluble protein recovery.

An unusual result was that there was an optimum transmembrane pressure for maximum observed transmission. Analysis using a simple "film-gel" model indicated that this peak in observed transmission was due to increases in wall concentration combined with a reduction in intrinsic transmission. Much more work is needed, however, before a full understanding is reached of the mechanisms which control flux, and particularly transmission, in crossflow filtration of a complex feedstream.

ACKNOWLEDGMENT

UCL is the Biotechnology and Biological Sciences Research Council's Advanced Centre for Biochemical Engineering, and the Council's support is gratefully acknowledged.

REFERENCES

1. C. S. Parnham III and R. H. Davis, "Protein Recovery from Cell Debris Using Rotary and Tangential Crossflow Microfiltration," *Biotechnol. Bioeng.*, *47*, 155–164 (1995).
2. A. I. Clarkson, M. Bulmer, and N. J. Titchener-Hooker, "Pilot-Scale Verification of a Computer-Based Simulation for Fractional Protein Precipitation," *Bioprocess Eng.*, *14*(2), 69–80 (1996).
3. K. H. Kroner, H. Schütte, H. Hustedt, and M.-R. Kula, "Crossflow Filtration in Downstream Processing of Enzymes," *Process Biochem.*, *19*(2), 67–74 (1984).
4. A. C. Bentham, M. J. Ireton, M. Hoare, and P. Dunnill, "Protein Precipitate Recovery Using Microporous Membranes," *Biotechnol. Bioeng.*, *31*, 984–994 (1988).
5. H. O. Bergmeyer, *Methods of Enzymatic Analysis*, Verlag Chemie, Weinham, 1983.
6. P. Milburn, J. Bonnerjea, M. Hoare, and P. Dunnill, "Selective Flocculation of Nucleic Acids, Lipids, and Colloidal Particles from a Yeast Cell Homogenate by Polyethyleneimine, and Its Scale Up," *Enzyme Microbiol. Technol.*, *12*, 527–532 (1990).
7. G. Belfort, R. H. Davis, and A. L. Zydney, "The Behaviour of Suspensions and Macromolecular Solutions in Crossflow Microfiltration," *J. Membr. Sci.*, *96*(1-2), 1–58 (1994).
8. S. M. Forman, E. R. DeBernardez, R. S. Feldberg, and R. W. Swartz, "Crossflow Filtration for the Separation of Inclusion Bodies from Soluble Proteins in Recombinant *Escherichia coli* Cell Lysate," *Ibid.*, *48*, 263–279 (1990).
9. M. C. Porter, "Concentration Polarization with Membrane Ultrafiltration," *Ind. Eng. Chem., Prod. Res. Dev.*, *11*(3), 234–248 (1972).
10. C. W. van Oers, M. A. G. Vorstman, W. G. H. M. Muijselgar, and P. J. A. M. Kerkhof, "Unsteady State Flux Behaviour in Relation to the Presence of a Gel Layer," *J. Membr. Sci.*, *73*(2-3), 231 (1992).
11. P. Aimar and R. W. Field, "Limiting Flux in Membrane Separations. A Model Based on the Viscosity Dependency of Mass Transfer Coefficient," *Chem. Eng. Sci.*, *47*(3), 579–586 (1992).
12. A. G. Fane, "Ultrafiltration, Factors Influencing Flux and Rejection," in *Progress in Filtration and Separation*, *Vol. 4* (R. J. Wakeman, Ed.), Elsevier Science, Amsterdam, 1986.

MARCEL DEKKER, INC.
270 Madison Avenue, New York, New York 10016

13. C. A. Romero and R. H. Davis, "Global Model of Crossflow Microfiltration Based on Hydrodynamic Diffusion," *J. Membr. Sci.*, *39*, 157–185 (1988).
14. G. Green and G. Belfort, "Fouling of Ultrafiltration Membranes, Lateral Migration and the Particle Trajectory Model," *Desalination*, *35*, 129–147 (1980).
15. R. K. Warren, D. G. MacDonald, and G. A. Hill, "Cross-Flow Microfiltration of *Saccharomyces cerevisiae*," *Process Biochem.*, *26*(6), 337–342 (1991).
16. G. Taylor, J. A. Levesley, and M. Hoare, "Pilot-Scale Ultrafiltration of Concentrated Protein Precipitate Suspensions: The Effect of Concentration and Fluid Dynamics, *Chem. Eng. Commun.*, *129*, 227–250 (1994).
17. G. P. Agarwal, "Analysis of Proteins Transmission in Vortex Flow Ultrafilter for Mass Transfer Coefficient," *J. Membr. Sci.*, *136*, 141–151 (1997).
18. K.-H. Kroner and V. Nissinen, "Dynamic Filtration of Microbial Suspensions Using an Annular Rotating Filter," *Ibid.*, *36*, 85–100 (1985).
19. R. Datar, "Studies on the Separation of Intracellular Soluble Enzymes from Bacterial Cell Debris by Tangential Flow Membrane Filtration," *Biotechnol. Lett.*, *7*(7), 471–476 (1985).
20. M. S. Le, L. B. Spark, and P. S. Ward, "The Separation of Aryl Acrylamidase by Cross Flow Microfiltration and the Significance of Enzyme Cell Debris Interaction," *J. Membr. Sci.*, *21*(3), 219–232 (1984).
21. C. Taddei, P. Aimar, G. Daufin, and V. Sanchez, "Mass Transfer during Sweet Whey Ultrafiltration on Mineral Membranes, *Lait*, *66*(4), 371–390 (1986).
22. G. Samuelsson, P. Dejmek, G. Tragardh, and M. Paulsson, "Minimising Whey Protein Retention in Cross-Flow Microfiltration of Skim Milk," *Int. Dairy J. 7*, 237–242 (1997).
23. M. Bennasar, D. Rouleau, R. Mayer, and B. T. de la Fuen, "Ultrafiltration of Milk on Mineral Membranes—Improved Performance," *J. Soc. Diary Technol.*, *35*(2), 43–49 (1982).
24. P. Blanpain, J. Hermia, and M. Lenoel, "Mechanisms Governing Permeate Flow and Protein Rejection in the Microfiltration of Beer with a Cyclopore Membrane," *J. Membr. Sci.*, *84*(1-2), 37 (1993).
25. M. S. Le and T. Atkinson, "Cross-Flow Microfiltration for Recovery of Intracellular Products," *Process Biochem.*, *20*(1), 26–31 (1985).
26. M. Balakrishnan and G. P. Agarwal, "Study of Protein Transmission through Ultrafiltration Membranes," *J. Membr. Sci.*, *85*(2), 111 (1993).
27. K. E. Göklen, M. Thien, S. Ayler, S. Smith, E. Fisher, M. Chartrain, P. Salmon, J. Wilson, A. Andrews, and B. Buckland, "Development of Crossflow Filtration Processes for the Commercial Isolation of a Bacterial Lipase," *Bioprocess Eng.*, *11*, 49–56 (1994).
28. W. R. Bowen and N. J. Hall, "Properties of Microfiltration Membranes: Mechanisms of Flux Loss in the Recovery of an Enzyme," *Biotechnol. Bioeng.*, *46*(1), 28 (1995).
29. J. A. Levesley and M. Hoare, "The Effect of High Frequency Backflushing on the Microfiltration of Yeast Homogenate Suspensions for the Recovery of Soluble Proteins," *J. Membr. Sci.*, *158*, 29–39 (1999).

Received by editor March 23, 1999
Revision received August 1999

Request Permission or Order Reprints Instantly!